arXiv:1404.1001v1 [hep-ph] 3 Apr 2014

April 4, 2014

$\bar{B}_s \to K$ semileptonic decay from an Omnès improved constituent quark model

C. Albertus,[1] E. Hernández,[2] C. Hidalgo-Duque,[3] and J. Nieves[3]

[1] *Departamento de Física Atómica, Nuclear y Molecular e Instituto Carlos I de Física Teórica y Computacional Universidad de Granada, Avenida de Fuentenueva s/n, E-18071 Granada, Spain.*

[2] *Departamento de Física Fundamental e IUFFyM, Universidad de Salamanca, Plaza de la Merced s/n, E-37008 Salamanca, Spain.*

[3] *Instituto de Física Corpuscular (IFIC), Centro Mixto CSIC-Universidad de Valencia, Institutos de Investigación de Paterna, Apartado 22085, E-46071 Valencia, Spain*

We study the f^+ form factor for the semileptonic $\bar{B}_s \to K^+ \ell^- \bar{\nu}_\ell$ decay in a constituent quark model. The valence quark estimate is supplemented with the contribution from the $\bar{B}^*$ pole that dominates the high q^2 region. We use a multiply-subtracted Omnès dispersion relation to extend the quark model predictions from its region of applicability near $q^2_{\rm max} = (M_{B_s} - M_K)^2 \sim 23.75$ GeV^2 to all q^2 values accessible in the physical decay. To better constrain the dependence of f^+ on q^2, we fit the subtraction constants to a combined input from previous light cone sum rule [Phys. Rev. D **78** (2008) 054015] and the present quark model results. From this analysis, we obtain $\Gamma(\bar{B}_s \to K^+ \ell^- \bar{\nu}_\ell) = (5.45^{+0.83}_{-0.80}) |V_{ub}|^2 \times 10^{-9}$ MeV, which is about 20% higher than the prediction based only on QCD light cone sum rule estimates. Differences are much larger for the f^+ form factor in the region above $q^2 = 15$ GeV^2.

PACS numbers: 12.15.Hh, 12.39.Jh, 13.20.He

I. INTRODUCTION

The magnitude of the V_{ub} element of the Cabibbo-Kobayashi-Maskawa (CKM) quark mixing matrix plays a critical role in testing the consistency of the Standard Model (SM) of particle physics and, in particular, the description of CP violation. Any inconsistency could be a sign of new physics beyond the SM. V_{ub} is currently the least well-known element of the CKM matrix and improvement in the precision of its determination is highly desirable and topical. At present, there exist some tension between the $|V_{ub}|$ values extracted from the analysis of inclusive decays and those from the study of exclusive channels. Thus, for instance, BABAR measurements of the inclusive electron and photon spectra in the $B \to X_u e\nu_e$ and $B \to X_s\gamma$ decays were used in Ref. [1] to extract $|V_{ub}|$ from data. Two different methods were used that led to two different values for the magnitude of the CKM matrix element V_{ub}, $(4.28 \pm 0.29 \pm 0.29 \pm 0.26 \pm 0.28) \times 10^{-3}$ and $(4.40 \pm 0.30 \pm 0.41 \pm 0.23) \times 10^{-3}$, respectively. These estimates could be compared with the value of $(3.41^{+0.37}_{-0.32}|_{\rm th} \pm 0.06|_{\rm exp}) \times 10^{-3}$ obtained in Ref. [2] from the exclusive semileptonic $B \to \pi$ form factors computed in QCD light cone sum rules (LCSR) for $q^2 < 12$ GeV^2 and the latest BABAR data available at the time.

In general, the determinations based on inclusive semileptonic decays using different calculational ansätze are consistent. The largest parametric uncertainty comes from the error on the $b-$quark mass. The PDG 2013 update [3] (review by R. Kowalewski and T. Mannel) quotes an inclusive average $|V_{ub}| = (4.41 \pm 0.15^{+0.15}_{-0.17}) \times 10^{-3}$. The value obtained from exclusive determinations, largely dominated by the semileptonic $B \to \pi$ decay, and quoted in [3] is $|V_{ub}| = (3.23 \pm 0.31) \times 10^{-3}$, where the precision is limited by form factor normalizations[1]. The two determinations are independent, but are marginally consistent with each other (see also the discussion and averages provided by the heavy flavor averaging group (HFAG) in [7][2]). On the other hand, $|V_{ub}|$ is also determined by the UTfit collaboration [9] from the unitarity triangle analysis within the SM. The tension between exclusive and inclusive determinations of the $|V_{ub}|$ CKM matrix element is now playing a major role in these SM fits because of the increased accuracy on several of the fundamental constraints [10].

Given the poor consistency between the inclusive and exclusive determinations, any new determination of $|V_{ub}|$ is then of the utmost importance. In this letter, we study the semileptonic decay $\bar{B}_s \to K^+\ell^-\bar{\nu}_\ell$. This decay channel is expected to be observed at LHCb and Belle and it could be used to get an independent determination of $|V_{ub}|$.

The semileptonic $\bar{B}_s \to K$ decay was analyzed in Refs. [11, 12] using LCSR and the relevant form factors were determined in the low q^2 region. Very recently, preliminary lattice QCD (LQCD) estimates for those form factors for higher q^2 values in the vicinity of $q^2_{\rm max} = (M_{B_s} - M_K)^2$ have become available [13], and a new wave of theoretical studies on some QCD-motivated models [14–17] have appeared as well. Parameterizations of the relevant form factor f^+ are provided by the relativistic quark (RQM), covariant light-front quark (LFQM) models and the perturbative (PQCD) approach of Refs. [14], [15] and [17], respectively. These were used in Ref. [6] to compute and compare the different predictions for the differential and partially integrated decay widths for $\bar{B}_s \to K^+\ell^-\bar{\nu}_\ell$, $\ell = e, \mu$ and $\ell = \tau$ decays, as well as some forward-backward asymmetry and the polarization fraction for the τ lepton. Conclusions however turned out to be inconclusive, because of the large discrepancies among the predictions from the different models considered.

Here we intend to obtain an improved description of the f^+ form factor in the whole q^2 range accessible, $[0, q^2_{\rm max}]$, in the decay and use it to predict the decay width ($\ell = e, \mu$) in units of $|V_{ub}|^2$. We follow the strategy of earlier work in Ref. [18], where we analyzed the semileptonic $B \to \pi$, $D \to \pi$ and $D_s \to K$ decays, and we use the quark model to evaluate the valence plus $\bar{B}^*$-pole contribution to the form factors. In this way we will derive reliable f^+ form factor values for high q^2, where the $\bar{B}^*$-pole contribution dominates, in good agreement with the LQCD results reported in [13] and the RQM calculation of Ref. [14]. Predictions in this region of the PQCD (LFQM) approach differ from ours by more than a factor of 3 (10). Our estimates for f^+ are however not accurate in the low q^2 region where the recoil of the final kaon is large. On the other hand, LCSR results, though trustful in the vicinity of $q^2 = 0$, cannot be used to describe f^+ above 10 GeV^2. We will then adopt the scheme of Refs. [19–21] and we shall take a multiply subtracted Omnès functional ansatz for the dominant f^+ form factor and will make a combined fit to our quark model results in the high q^2 region and to the LCSR results in the low q^2 region. The Omnès representation is employed to provide a parameterization of the form factor constrained by unitarity and analyticity properties. In this way, we obtain a determination of the form factor in accordance with LCSR and lattice results, that can be used to determine the decay width. For low and intermediate q^2 values, discrepancies with the PQCD and LFQM approaches are not as dramatic as in the vicinity of $q^2_{\rm max}$, though they are still significant, while some disagreement with the RQM predictions show up now, that lead to a totally integrated width around 20% larger in this work than that reported in [14].

---

[1] The value obtained from the semileptonic exclusive $B \to \rho$ decay is even smaller by around 20% [4, 5]. However, it has been recently pointed out [6] that $\pi\pi$ distribution effects in the broad $\rho-$width, not considered in [4, 5], might lead to an enhanced $|V_{ub}|$ value determined from this decay mode.

[2] A complete listing of the averages and plots, including updates since [7] was prepared, are also available on the HFAG web site [8].

II. SEMILEPTONIC $\bar{B}_s \to K$ DECAY

For a $0^- \to 0^-$ transition, the weak hadronic matrix element can be parameterized as

$$\langle K^+,\, \vec{p}_K\, |\bar{\Psi}_u(0)\gamma^\mu(1-\gamma_5)\Psi_b(0)|\bar{B}_s,\, \vec{p}\rangle = \Big(P^\mu - q^\mu \frac{M_{B_s}^2 - M_K^2}{q^2}\Big) f^+(q^2) + q^\mu \frac{M_{B_s}^2 - M_K^2}{q^2} f^0(q^2) \tag{1}$$

with $P = p + p_K$, $q = p - p_K$ and where $f^+(q^2), f^0(q^2)$ are form factors. In the case of small lepton masses ($l = e, \mu$) the part proportional to q^μ gives a very small contribution, when contracted with the leptonic current, and it can safely be neglected. Only the $f^+(q^2)$ form factor would play a role in the decay.

For zero lepton masses, the differential decay width is in fact given by

$$\frac{d\Gamma}{dq^2} = \frac{G_F^2}{192\pi^3}\,|V_{ub}|^2\,\frac{\lambda^{3/2}(q^2, M_{B_s}^2, M_K^2)}{M_{B_s}^3}\,|f^+(q^2)|^2 \tag{2}$$

with $G_F = 1.166378 \times 10^{-5}\,\mathrm{GeV}^{-2}$ the Fermi decay constant and $|V_{ub}|$ the modulus of the corresponding Cabibbo-Kobayashi-Maskawa matrix element. λ is the Källen function defined as $\lambda(a,b,c) = a + b^2 + c^2 - 2ab - 2ac - 2bc$.

A. Valence contribution to the form factors

For a $\bar{B}_s$ meson initially at rest and taking $\vec{q}$ in the positive Z direction ($\vec{q} = |\vec{q}|\vec{k}$), the valence quark model contribution to the form factors is evaluated as [22]

$$\begin{aligned} f^+(q^2) &= \frac{1}{2M_{B_s}}\,\left[V^0(|\vec{q}|) + \frac{V^3(|\vec{q}|)}{|\vec{q}|}\,(E_K(-\vec{q}) - M_{B_s})\right] \\ f^0(q^2) &= \frac{1}{2M_{B_s}}\,\left\{V^0(|\vec{q}|)\,\frac{q^2 + M_{B_s}^2 - M_K^2}{M_{B_s}^2 - M_K^2} + \frac{V^3(|\vec{q}|)}{|\vec{q}|}\,\left[E_K(-\vec{q})\frac{q^2 + M_{B_s}^2 - M_K^2}{M_{B_s}^2 - M_K^2} + M_{B_s}\frac{q^2 - M_{B_s}^2 + M_K^2}{M_{B_s}^2 - M_K^2}\right]\right\} \end{aligned} \tag{3}$$

with V^0 and V^3 the following vector matrix elements

$$\begin{aligned} V^0(|\vec{q}|) = \sqrt{2M_{B_s}2E_K(-\vec{q})}\;&\int d^3p\;\frac{1}{4\pi}\Phi_K^*(|\vec{p}|)\,\Phi_{B_s}\left(\left|\vec{p} - \frac{m_s}{m_u+m_s}|\vec{q}|\vec{k}\right|\right) \\ &\sqrt{\frac{\widehat{E}_u\widehat{E}_b}{4E_uE_b}}\left(1 + \frac{(-\frac{m_u}{m_u+m_s}\,|\vec{q}|\vec{k} - \vec{p})\cdot(\frac{m_s}{m_u+m_s}\,|\vec{q}|\vec{k} - \vec{p})}{\widehat{E}_u\widehat{E}_b}\right) \\ V^3(|\vec{q}|) = \sqrt{2M_{B_s}2E_K(-\vec{q})}\;&\int d^3p\;\frac{1}{4\pi}\Phi_{B_s}\left(\left|\vec{p} - \frac{m_s}{m_u+m_s}|\vec{q}|\vec{k}\right|\right) \\ &\sqrt{\frac{\widehat{E}_u\widehat{E}_b}{4E_uE_b}}\left(\frac{\frac{m_s}{m_u+m_s}\,|\vec{q}| - p_z}{\widehat{E}_b} + \frac{-\frac{m_u}{m_u+m_s}\,|\vec{q}| - p_z}{\widehat{E}_u}\right) \end{aligned} \tag{4}$$

Here $E_u = E_u(-\frac{m_u}{m_u+m_s}\,|\vec{q}|\vec{k} - \vec{p}), E_b = E_b(\frac{m_s}{m_u+m_s}\,|\vec{q}|\vec{k} - \vec{p})$ while $\widehat{E}_q = E_q + m_q$. The wave functions (Fourier transforms of the radial coordinate space $\bar{B}_s$ and K meson wave functions, which describe the relative dynamics of the quark-antiquark pair) are evaluated using the AL1 interquark potential of Refs. [23, 24]. This potential contains a linear confinement term plus $1/r$ and hyperfine terms coming from one-gluon exchange. The masses and the rest of the parameters were fitted in Ref. [23] to reproduce the light and heavy-light meson spectra.

In the left panel of Fig 1 we show the results for the form factors thus obtained. These form factors are not correct in the high q^2 region where the pole of the $\bar{B}^*$ makes the largest contribution, and they are also incorrect at low q^2 where the recoil of the final meson is largest. We shall improve their behavior in both regions

B. $\bar{B}^*$-pole contribution to the form factors.

The Feynman diagram for the $\bar{B}^*$-pole contribution to the decay process appears in Fig. 2. The corresponding weak matrix element is given by [18]

$$g_{B^*B_sK}(q^2)\sqrt{q^2}f_{B^*}(q^2)\,\frac{p_K^\mu - q^\mu(p_K\cdot q)/M_{B^*}^2}{M_{B^*}^2 - q^2} \tag{5}$$

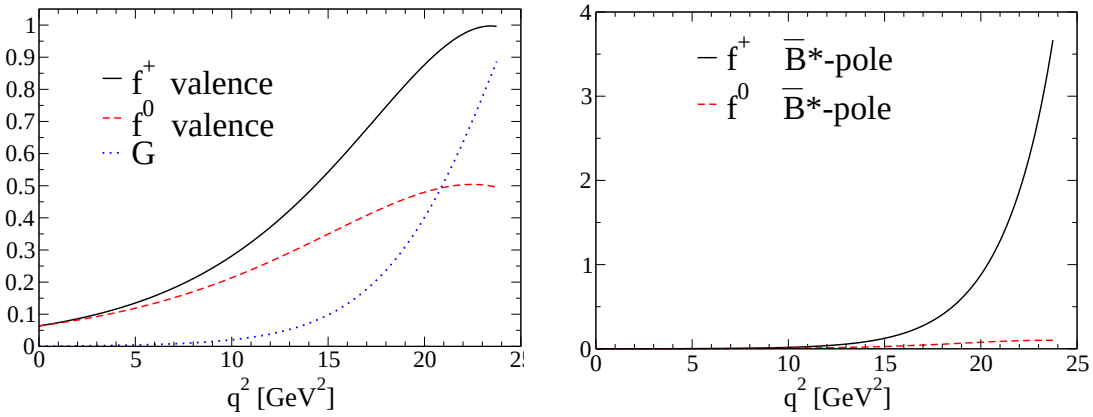

FIG. 1. Left panel: Valence quark contribution to the $f^+(q^2)$ and $f^0(q^2)$ form factors and the $G(q^2)$ function as defined in Eq.(10). Right panel: $\bar{B}^*$-pole contribution to the $f^+(q^2)$ and $f^0(q^2)$ form factors evaluated in the constituent quark model.

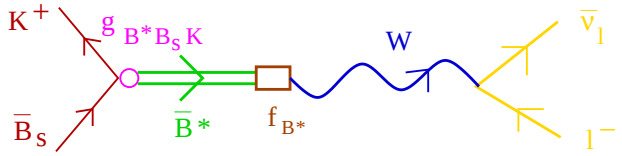

FIG. 2. Feynman diagram corresponding to the $\bar{B}^*$-pole contribution to the $\bar{B}_s \to K$ semileptonic decay.

from where

$$f^+_{\rm pole}(q^2) = \frac{g_{B^*B_sK}(q^2)}{2}\sqrt{q^2} f_{B^*}(q^2)\frac{1}{M^2_{B^*}-q^2}, \tag{6}$$

$$f^0_{\rm pole}(q^2) = \frac{g_{B^*B_sK}(q^2)}{2}\sqrt{q^2} f_{B^*}(q^2)\frac{M^2_{B_s}-M^2_K-q^2}{(M^2_{B_s}-M^2_K)M^2_{B^*}} \tag{7}$$

Within the quark model we have that [27]

$$f_{B^*}(q^2) = \frac{\sqrt{6}}{(q^2)^{1/4}\,\pi}\int_0^\infty d|\vec{p}\,|\Phi_{B^*_u}(|\vec{p}\,|)\,|\vec{p}\,|^2\sqrt{\frac{\widehat{E}_b\widehat{E}_u}{4E_bE_u}}\left(1+\frac{|\vec{p}\,|^2}{3\widehat{E}_b\widehat{E}_u}\right) \tag{8}$$

$$= f_{B^*}\sqrt{\frac{M_{B^*}}{\sqrt{q^2}}} \tag{9}$$

with $E_q = E_q(|\vec{p}\,|) = \sqrt{m_q^2+\vec{p}^{\,2}}$, $\widehat{E}_q = E_q + m_q$, and where f_{B^*} is the on-shell decay constant for which we get $f_{B^*} = 151\,\text{MeV}$ [27]. Finally $g_{B^*B_sK}(q^2)$ is obtained as explained in Ref. [27]. We write it as

$$g_{B^*B_sK}(q^2) = g_{B^*B_sK}\,G(q^2) \tag{10}$$

where $g_{B^*B_sK}$ is the B^*B_sK coupling constant evaluated at $q^2 = M^2_{B^*}$ but in the chiral limit (zero kaon mass). We get for its value $g_{B^*B_sK} = 49.88$. The $G(q^2)$ function is a dimensionless hadronic factor normalized to one at $q^2 = M^2_{B^*}$, which accounts for the q^2 dependence of $\bar{B}_s \to \bar{B}^*K$ amplitude. It is shown in the left panel of Fig. 1. The product $g_{B^*B_sK}\,f_{B^*}$ is given in our model as

$$g_{B^*B_sK}\,f_{B^*} = 7.53\,\text{GeV} \tag{11}$$

This value is too large compared to the LCSR determination of Ref. [11]. There the authors get values in the range $g_{B^*B_sK}\,f_{B^*} = 3.57-4.19\,\text{GeV}$. On the other hand one can make use of SU(3) symmetry to get the relation [28]

$$g_{B^*B_sK}\,f_{B^*} = g_{B^*B\pi}\,f_{B^*}\sqrt{\frac{M_{B_s}}{M_B}}\frac{f_\pi}{f_K} \tag{12}$$

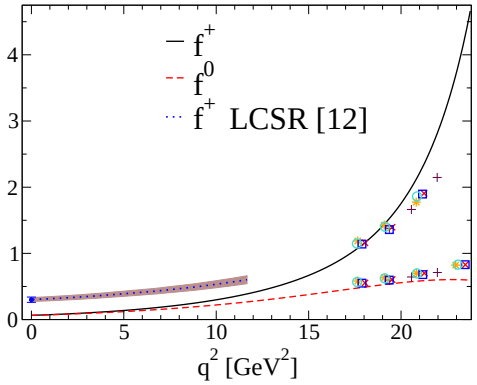

FIG. 3. Total, valence plus $\bar{B}^*$-pole contributions, $f^+(q^2)$ and $f^0(q^2)$ form factors. We also show the results obtained in the LCSR calculation of Ref. [12] (dotted-line plus error band) and different preliminary lattice data in the high q^2 region reported in Ref. [13].

Lattice data for f_{B^*} [29] and $g_{B^*B\pi}$ [30] gives $g_{B^*B\pi}\, f_{B^*} = 8.9 \pm 2.2\,\text{GeV}$, from where SU(3) symmetry will predict

$$g_{B^*B_sK}\, f_{B^*} = 7.49 \pm 1.85\,\text{GeV} \tag{13}$$

in good agreement with our determination. We shall use this latter result and the error will serve to evaluate the uncertainties in our quark model calculation. The $\bar{B}^*$-pole contribution to the form factors using $g_{B^*B_sK}\, f_{B^*} = 7.49\,\text{GeV}$ is presented in the right panel of Fig. 1.

The total quark model form factors, valence plus $\bar{B}^*$-pole contributions, are shown in Fig. 3. There, we also show the results of the LCSR calculation of Ref. [12] (very similar results, not shown, are obtained in Ref. [11]), and preliminary LQCD results for high q^2 obtained in Ref. [13] with different lattice configurations. In the LCSR approach of Ref. [12] a value of $f^+(0) = 0.30^{+0.04}_{-0.03}$ is reported and we have assumed a similar 10% error on the LCSR form factor at larger q^2 that we show as an error band in Fig. 3. Our results are compatible with lattice data if one takes into account the uncertainties in the $g_{B^*B_sK}\, f_{B^*}$ value. However, the disagreement with the LCSR results in the low q^2 region can not be corrected in that way. The quark model evaluation is not appropriate for low q^2 where the kaon recoil is large. In the next subsection we shall use the Omnès representation to combine our quark model results, that we consider to be reliable in the high q^2 region, with the LCSR results in the low q^2 part. In this way we shall get a realistic description of the form factor for all q^2 values allowed in the decay.

C. Omnès representation of the f^+ form factor

Here we shall use the multiply subtracted Omnès representation of the f^+ form factor as discussed in Ref. [20], where the $\bar{B}^*$-pole has been made explicit

$$f^+(q^2) \approx \frac{1}{M^2_{B^*} - q^2} \prod_{j=0}^{n} \left[f^+(q^2_j)\Big(M^2_{B^*} - q^2_j\Big)\right]^{\alpha_j(q^2)} \tag{14}$$

$$\alpha_j(q^2) = \prod_{j\neq k=0}^{n} \frac{q^2 - q^2_K}{q^2_j - q^2_k} \tag{15}$$

with $q^2 < s_{\rm th} = (M_{B_s} + M_K)^2$ and $q_0, \cdots q^2_n \in]-\infty, s_{\rm th}[$, the q^2-values where the $(n+1)$ subtractions are considered. In addition, $f^+(q^2_j)$ are the values that the form factor takes at the subtraction points. The Omnès representation above emerges from Watson's theorem that states,

$$\frac{f^+(s+i\epsilon)}{f^+(s-i\epsilon)} = e^{2i\delta(s)}, \qquad s \geq s_{\rm th} \tag{16}$$

where $\delta(s)$ is the phase-shift for elastic $K\bar{B}_s \to K\bar{B}_s$ scattering in the total angular momentum $J = 1$ channel. In principle, the Omnès representation requires as an input the phase shift plus the form factor at $(n+1)$ positions $\{q^2_i\}$ values below the $K\bar{B}_s$ threshold. For sufficiently many subtractions, the phase shift $\delta(s)$ can be approximated by its

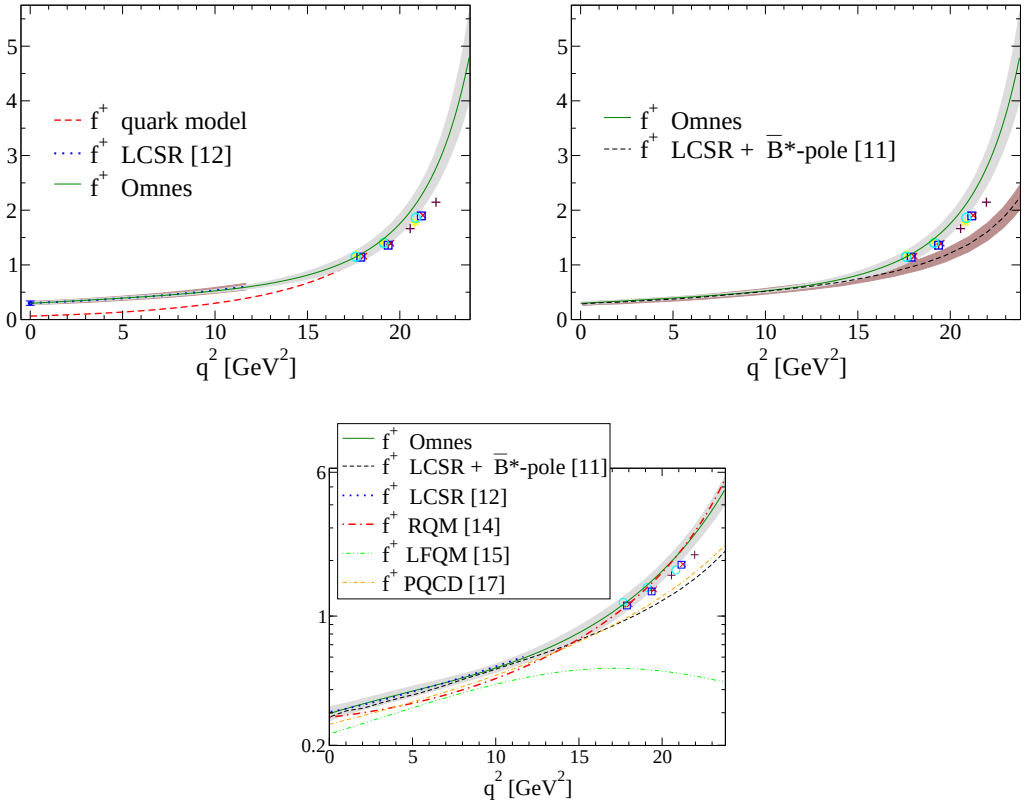

FIG. 4. Upper-left panel: $f^+(q^2)$ evaluated in the quark model (red dashed line) and improved at lower q^2 by means of the Omnès representation (solid line plus 68% confidence level band). We also show the LCSR results of Ref. [12] (blue dotted-line+10% error band) and different preliminary lattice data taken from Ref. [13]. Upper-right panel: We compare our final result (solid line plus 68% confidence level band) with the fit in Ref. [11] (dashed-line). For the latter a 10% error band is also displayed. Lattice data points taken from Ref. [13] are also shown. Lower panel: Global comparison of our final result for the f^+ form factor with different calculations using LCSR [12], LCSR+$\bar{B}^*$-pole fit [11], RQM [14], LFQM [15] and PQCD [17]. Lattice data from Ref. [13] are also shown for comparison.

value at threshold[3] leading to the approximate representation of Eq. (14). This amounts to finding an interpolating polynomial for $\ln\left[(M_{B^*}^2 - q^2)f^+(q^2)\right]$ passing through the points $\ln\left[(M_{B^*}^2 - q_i^2)f^+(q_i^2)\right]$. While one could always propose a parametrization using an interpolating polynomial for $\ln\left[g(q^2)f^+(q^2)\right]$ for a suitable function $g(q^2)$, the derivation in [20] using the Omnès representation shows that taking $g(q^2) = (M_{B^*}^2 - q^2)$ is physically motivated.

The approach that we shall follow is the one in Ref. [21]. Taking for q_j^2 the four different values 0, $q^2_{\rm max}/3$, $2q^2_{\rm max}/3$ and $q^2_{\rm max}$, we treat $f^+(q_j^2)$ as free parameters and make a combined χ^2-fit to our quark model results and the LCSR predictions of Ref. [12] in the high and low q^2 regions, respectively. We take LCSR values for f^+ at $q^2 = 0, 2, 4, 6, 8$ and 10 GeV^2 with a 10% relative error, as mentioned above, while we fit to our quark model results for $q^2 = 19, 20, 21, 22$ and 23 GeV^2, and assign to these points the error that derives from using $g_{B^*B_sK}\, f_{B^*} = 7.49 \pm 1.85\,$GeV.

The outcome of the fit is

$$\begin{aligned} f^+(0) &= 0.297 \pm 0.026, \\ f^+(q^2_{\rm max}/3) &= 0.460 \pm 0.025, \\ f^+(2\,q^2_{\rm max}/3) &= 0.896 \pm 0.084, \\ f^+(q^2_{\rm max}) &= 4.792 \pm 0.808 \end{aligned} \tag{17}$$

and the corresponding form factor, together with a 68% confidence level band, is depicted in the upper-left panel of Fig. 4. The procedure to build the 68% confidence level band for the form factor is the following: We generate a 1000 sets of $(f^+(0), f^+(q^2_{\rm max}/3), f^+(2\,q^2_{\rm max}/3), f^+(q^2_{\rm max}))$ values assuming an uncorrelated four-dimensional Gaussian

[3] It is set to zero, with the help of Levinson's theorem (see the detailed discussion in Ref. [20]).

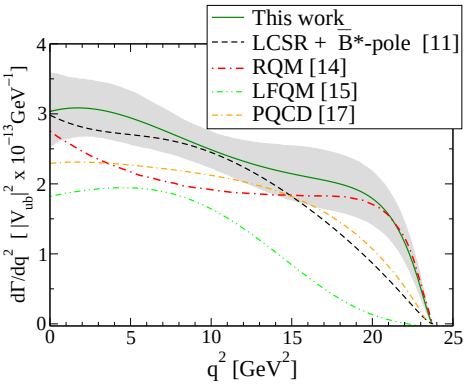

FIG. 5. Differential decay width obtained in this work with the Omnès fit (solid line plus 68% confidence level band) and in LCSR+$\bar{B}^*$-pole fit [11], RQM [14], LFQM [15] and PQCD [17] approaches.

	This work	LCSR+$\bar{B}^*$-pole [11]	RQM [14]	LFQM [15]	PQCD [17]
$\Gamma\ [\,\lvert V_{ub}\rvert^2 \times 10^{-9}\,\text{MeV}]$	$5.45^{+0.83}_{-0.80}$	$4.63^{+0.97}_{-0.88}$	4.50 ± 0.55	3.17 ± 0.24	4.2 ± 2.1

TABLE I. Decay width in units of $|V_{ub}|^2 \times 10^{-9}$ MeV from several approaches. For the result of Ref. [11] we have propagated a 10% uncertainty in the form factor. Results for Refs. [14, 15, 17] have been adapted from Table IV in Ref. [6].

distribution for which the central values and the standard deviations are taken from Eq. (17). In this way we generate a 1000 different f^+ form factors. The 68% confidence level band is built discarding for each q^2 the 16% largest and 16% lowest values of the form factor.

A different fit was performed in Ref. [11]. There, a value of $g_{B^*B_sK}f_{B^*} = 3.88 \pm 0.31\,\text{GeV}$ was used and as a consequence the form factor extracted in [11] is very different from ours for large q^2-values, where the $\bar{B}^*$-pole contribution dominates. A comparison of the two form factors is given in the upper-right panel of Fig. 4.

In the lower panel of Fig. 4 we compare the f^+ form factor as calculated in different approaches. The LCSR calculation of Ref. [12] only provides results up to $q^2 = 10\,\text{GeV}^2$ and the PQCD calculation of Ref. [17] does not include a $\bar{B}^*$-pole contribution and then its form factor is not reliable in the high q^2 region. All other calculations do include the $\bar{B}^*$-pole mechanism, but they differ in its strength. The RQM calculation of Ref. [14] provides a result similar to ours in the region of q^2 dominated by the $\bar{B}^*$-pole, while Refs. [11, 17] give smaller values. Lattice data in the high q^2 region will be most valuable to decide which of the two sets of calculations is more correct. As seen in the figure there are also differences in the low q^2 part that will get amplified in the differential decay width.

D. Prediction for the decay width

With the Omnès form factor, we evaluate the differential decay width that is displayed in Fig. 5, together with its 68% confidence level band. We also show the differential decay width that derives from the calculations in Refs. [11, 14, 15, 17]. The differences present in the form factors at low and high q^2 have a clear reflection here.

For the integrated decay width we finally obtain

$$\Gamma(\bar{B}_s \to K^+\ell^-\bar{\nu}_\ell) = (5.45^{+0.83}_{-0.80})|V_{ub}|^2 \times 10^{-9}\,\text{MeV} \tag{18}$$

A comparison with the other approaches is given in Table I. The calculations in Refs. [11, 14] predict very similar results, even though their form factors deviate both in the low and high q^2 region, but whose effects compensate in the integrated width. The result of the PQCD calculation of Ref. [17] is also similar, but in that case the uncertainty, as quoted in Ref. [6], is around 50%. A smaller result is given in the LFQM calculation of Ref. [15]. This is in part a reflection of the fact that no $\bar{B}^*$- pole contribution is included in that approach. Our result is the largest although we agree with Refs. [11, 14, 17] within uncertainties.

One might be tempted to combine[4] our result with the ones in Refs. [11, 14]. In that case, one would get

$$\Gamma(\bar{B}_s \to K^+\ell^+\bar{\nu}_\ell) = (4.77 \pm 0.41)|V_{ub}|^2 \times 10^{-9}\,\mathrm{MeV} \tag{19}$$

Once experimental data is available, the above result may be used to obtain the value of $|V_{ub}|$ with a theoretical error of the order of 5%. Nevertheless, we believe that our estimate for $\Gamma(\bar{B}_s \to K^+\ell^-\bar{\nu}_\ell)$ in Eq. (18) is more accurate. The RQM approach at low and intermediate values of q^2 should not be as appropriated as the LCSR scheme, whose input is included in our combined scheme. Conversely, our quark model predictions for f^+ agree remarkably well with those of the RQM of Ref. [14] at high q^2 values, and are significantly larger than those provided by the $\bar{B}^*$ pole contribution assumed in [11]. Indeed, the value for $g_{B^*B_sK}f_{B^*}$ used in that work strongly disagrees, both with our predictions and with the existing LQCD data. Moreover, the agreement showed in Table I among Refs. [11, 14] is just a coincidence, because their respective predictions for $f^+(q^2)$ and $d\Gamma/dq^2$ in Figs. 4 (bottom panel) and 5 significantly differ for most of the available phase space.

III. SUMMARY

We have studied the form factor f^+ for the semileptonic $\bar{B}_s \to K^+\ell^-\bar{\nu}_\ell$ decay within an Omnès scheme, which incorporates unitarity and analyticity constrains and it makes possible to combine quark model and LCSR results in the high and low q^2 regions, respectively. We predict $\Gamma(\bar{B}_s \to K^+\ell^-\bar{\nu}_\ell)$ with a theoretical uncertainty of the order of 15%, inherited from the 10% and 25% errors on the LCSR and quark model inputs for f^+, respectively. Uncertainties on the predicted differential width (Fig. 5) turn also to be moderately small. Once experimental data is available, our prediction for $\Gamma(\bar{B}_s \to K^+\ell^-\bar{\nu}_\ell)$ in Eq. (18) or $d\Gamma/dq^2$ could be used to determine $|V_{ub}|$ with a theoretical error of the order of 7%, which will be reduced by improved LCSR and LQCD results. In particular, LQCD simulations could not only provide the form factor f^+, that could be directly fitted, but also a more accurate determination of $g_{B^*B_sK}f_{B^*}$, which is the major source of uncertainty in the quark model input included in the combined Omnès analysis. Experimental data for this reaction is expected from the LHCb and Belle Collaborations in the near future.

ACKNOWLEDGMENTS

This research was supported by the Spanish Ministerio de Economía y Competitividad and European FEDER funds under Contracts Nos. FPA2010-21750-C02-02, FIS2011-28853-C02-02, and the Spanish Consolider-Ingenio 2010 Programme CPAN (CSD2007-00042), by Generalitat Valenciana under Contract No. PROMETEO/20090090, by Junta de Andalucia under Contract No. FQM-225, by the EU HadronPhysics3 project, Grant Agreement No. 283286, and by the University of Granada start-up Project for Young Researches contract No. PYR-2014-1. C.A. wishes to acknowledge a CPAN postdoctoral contract and C.H.-D. thanks the support of the JAE-CSIC Program.

[1] V. B. Golubev, Y. I. Skovpen and V. G. Luth, Phys. Rev. D **76**, 114003 (2007).
[2] A. Khodjamirian, T. .Mannel, N. Offen and Y. -M. Wang, Phys. Rev. D **83**, 094031 (2011).
[3] J. Beringer *et al.* [Particle Data Group Collaboration], Phys. Rev. D **86** (2012) 010001.
[4] J. M. Flynn, Y. Nakagawa, J. Nieves and H. Toki, Phys. Lett. B **675**, 326 (2009).
[5] P. del Amo Sanchez *et al.* [BaBar Collaboration], Phys. Rev. D **83**, 032007 (2011).
[6] U. -G. Meißner and W. Wang, JHEP **1401**, 107 (2014).
[7] Y. Amhis *et al.* [Heavy Flavor Averaging Group Collaboration], arXiv:1207.1158 [hep-ex].
[8] `http://www.slac.stanford.edu/xorg/hfag`
[9] `http://www.utfit.org/UTfit/Results`
[10] A. Bevan, M. Bona, M. Ciuchini, D. Derkach, E. Franco, L. Silvestrini, V. Lubicz and C. Tarantino *et al.*, Nucl. Phys. Proc. Suppl. **241-242**, 89 (2013).
[11] Z. -H. Li, F. -Y. Liang, X. -Y. Wu and T. Huang, Phys. Rev. D **64**, 057901 (2001).
[12] G. Duplancic and B. Melic, Phys. Rev. D **78**, 054015 (2008).
[13] C. M. Bouchard, G. P. Lepage, C. J. Monahan, H. Na and J. Shigemitsu, arXiv:1310.3207 [hep-lat].
[14] R. N. Faustov and V. O. Galkin, Phys. Rev. D **87**, no. 9, 094028 (2013).

[4] We symmetrize the errors displayed in Table I and use the maximum likelihood method for which $\Gamma_{\rm avg}/\sigma^2 = \sum_i \Gamma_i/\sigma_i^2$, with $1/\sigma^2 = \sum_i 1/\sigma_i^2$.

[15] R. C. Verma, J. Phys. G **39** 025005 (2012).
[16] F. Su, Y. -L. Wu, C. Zhuang and Y. -B. Yang, Eur. Phys. J. C **72**, 1914 (2012).
[17] W. -F. Wang and Z. -J. Xiao, Phys. Rev. D **86**, 114025 (2012).
[18] C. Albertus, J. M. Flynn, E. Hernandez, J. Nieves and J. M. Verde-Velasco, Phys. Rev. D **72**, 033002 (2005).
[19] J. M. Flynn and J. Nieves, Phys. Rev. D **75**, 013008 (2007).
[20] J. M. Flynn and J. Nieves, Phys. Lett. B **649**, 269 (2007).
[21] J. M. Flynn and J. Nieves, Phys. Rev. D **76**, 031302 (2007).
[22] E. Hernandez, J. Nieves and J. M. Verde-Velasco, Phys. Rev. D **74**, 074008 (2006).
[23] C. Semay and B. Silvestre-Brac, Z. Phys. C **61**, 271 (1994).
[24] B. Silvestre-Brac, Few Body Syst. **20**, 1 (1996).
[25] C. Semay, and B. Silvestre-Brac, Z. Phys. C 61, 271 (1994).
[26] B. Silvestre-Brac, Few-Body Systems 20 (1996) 1.
[27] C. Albertus, E. Hernandez, J. Nieves and J. M. Verde-Velasco, Phys. Rev. D **71**, 113006 (2005).
[28] P. Colangelo and F. De Fazio, Phys. Lett. B **532**, 193 (2002)
[29] K. C. Bowler *et al.* [UKQCD Collaboration], Nucl. Phys. B **619**, 507 (2001).
[30] A. Abada, D. Becirevic, P. Boucaud, G. Herdoiza, J. P. Leroy, A. Le Yaouanc and O. Pene, JHEP **0402**, 016 (2004).